Biochemical and Biophysical Research Communications **261,** 123–130 (1999)
Article ID bbrc.1999.0984, available online at http://www.idealibrary.com on IDEAL®

# Reduced Mitochondrial Membrane Potential and Altered Responsiveness of a Mitochondrial Membrane Megachannel in p53-Induced Senescence

Mary M. Sugrue,*[,1] Yan Wang,* Hardy J. Rideout,† Ruth M. E. Chalmers-Redman,† and William G. Tatton†

*Department of Pediatrics, Division of Hematology/Oncology, and †Department of Neurology, Mount Sinai School of Medicine, One Gustave L. Levy Place, New York, New York 10029-6574*

Received June 9, 1999

**There is accumulating evidence that mitochondrial membrane potential ($\Delta\Psi_M$) is reduced in aged cells. In addition, a decrease of $\Delta\Psi_M$ has been shown to be an early event in many forms of apoptosis. Here we use a mitochondrial potentiometric dye with *in situ* laser scanning confocal microscopic (LSCM) imaging to demonstrate that $\Delta\Psi_M$ is dramatically decreased in both the p53-overexpressing, senescent EJ tumor cells and in pre-apoptotic PC12 cells compared to controls. Treatment with cyclosporin A (CSA), which facilitates closure of the mitochondrial permeability transition pore (PTP), was able to reverse the decrease in $\Delta\Psi_M$ in pre-apoptotic PC12 cells but not in the senescent EJ-p53 cells. The capacity to prevent dissipation of $\Delta\Psi_M$ in response to agents that facilitate PTP closure may differentiate cells entering apoptosis from those participating in senescence. Therefore, regulation of the closure of the mitochondrial PTP in the presence of decreased $\Delta\Psi_M$ may be a decisional checkpoint in distinguishing between growth arrest pathways.** © 1999 Academic Press

We previously showed that overexpression of wild-type p53 rapidly triggers a senescence program in EJ tumor cells (1). In addition to the characteristic features of the senescence phenotype, which included distinct morphological changes, irreversible growth arrest, senescence-associated β-galactosidase staining, and the accumulation of lipofuscin, the p53 overexpression was associated with a decrease in the density of mitochondrial cristae on electron microscopic (EM) examination. Overexpression of amyloid precursor protein (APP751) in P19 cells has also been shown to result in decreased density of mitochondrial cristae, which is associated with a decrease in mitochondrial membrane potential ($\Delta\Psi_M$) (2). Studies using a variety of mitochondrial potentiometric dyes have suggested that $\Delta\Psi_M$ is reduced in aged liver cells (3, 4), fibroblasts (5), lymphocytes (6–8) and cardiomyocytes (9). It is not known whether p53-induced senescence involves a similar decrease in $\Delta\Psi_M$.

A decrease in $\Delta\Psi_M$ is an early event in many forms of apoptosis (10), including those that involve p53 (11). Opening of a multi-protein mitochondrial membrane megachannel, the permeability transition pore (PTP, see refs. 12–14 for reviews) results in the dissipation of $\Delta\Psi_M$ with the release of intramitochondrial factors (15–18), which initiate apoptotic degradation (19). Cyclosporin A (CSA), which was the first agent used to identify a responsive element of the PTP (20, 21) and can be used to examine the effect of PTP closure on $\Delta\Psi_M$ (22, 23), prevents cyclophilin D from interacting with the adenine nucleotide translocator (ANT) and the voltage-dependent anion channel (VDAC) (24, 25) of the PTP and thereby, facilitates PTP closure and maintains or increases $\Delta\Psi_M$. Although, maintenance of PTP closure and $\Delta\Psi_M$ accompanies a decrease in some forms of apoptosis (16), it is not known whether the PTP participates in the decreased $\Delta\Psi_M$ found in aged or senescent cells.

In order to determine whether the changes in the density of mitochondrial cristae were associated with a change in $\Delta\Psi_M$, we measured $\Delta\Psi_M$ in the p53-overexpressing senescent cells and compared the $\Delta\Psi_M$

[1] To whom correspondence should be addressed. Fax: 212-426-1972. E-mail: m.sugrue@smtplink.mssm.edu.

Abbreviations used: $\Delta\Psi_M$, mitochondrial membrane potential; ANT, adenine nucleotide translocator; ATR, atractyloside; CMTMR, chloromethyl tetramethyl rosamine; CSA, cyclosporin A; LSCM, laser scanning confocal microscopy; MEM, minimum essential medium; M/O, MEM without serum or NGF; M/S + N, MEM with serum and NGF; NGF, nerve growth factor; PC12, pheochromocytoma cell; PTP, permeability transition pore; tet, tetracycline; VDAC, voltage-dependent anion channel.



0006-291X/99 $30.00

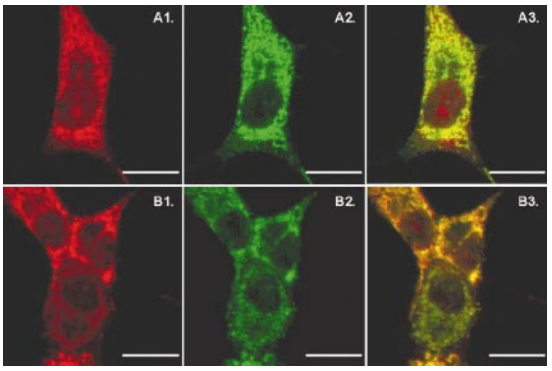


**FIG. 1.** Images of CMTMR fluorescence and biotin immunoreaction in partially neuronally differentiated vs. serum- and NGF-withdrawn (pre-apoptotic) PC12 cells. Laser scanning confocal microscopic (LSCM) images of neuronally differentiated PC12 cells, washed and then replaced in MEM with serum and NGF (A1, A2, A3), or washed and placed in MEM alone (serum- and NGF-withdrawn) to induce apoptosis (B1, B2, B3). A1 and B1 are images of cells stained with CMTMR that were collected as 8 bit gray scale images and digitally recolored red. A2 and B2 are images of cells immunoreacted for biotin that were also grayscale but recolored green. In the digitally added images (A3, B3), pure red or pure green would indicate an absence of biotin immunoreaction or CMTMR fluorescence, respectively. A progression from red-orange to orange to yellow to yellow-green indicates image pixels with an increasing preponderance of biotin immunoreaction but where biotin immunoreaction and CMTMR fluorescence are co-localized (as in A3 and B3). The images show that CMTMR fluorescence is only found in co-localization with the biotin mitochondrial marker. Note the lower level of CMTMR fluorescence in B2 as compared to B1 but the similarity of the levels of biotin immunofluorescence in A1 and A2, which parallels the predominance of yellow and yellow-green coloration in A3 and yellow-range fluorescence in B3. Also note the cell in B1 that has markedly decreased CMTMR fluorescence but retains biotin immunofluorescence. All scale bars are 10 $\mu$m in length.

measurements to those in pre-apoptotic PC12 cells using a $\Delta\Psi_M$-sensitive dye with *in situ* laser scanning confocal microscope (LSCM) imaging. We found a dramatic decrease in $\Delta\Psi_M$ in both the senescent EJ tumor cells and the pre-apoptotic PC12 cells, but not in control EJ tumor cells or non-apoptotic PC12 cells. CSA increased $\Delta\Psi_M$ in pre-apoptotic PC12 cells, non-apoptotic PC12 cells and control EJ tumor cells, but did not modify $\Delta\Psi_M$ in the p53-overexpressing, senescent EJ cells. The capacity to increase $\Delta\Psi_M$ in response to agents that induce PTP closure may differentiate cells entering apoptosis from those participating in a senescence program.

## MATERIALS AND METHODS

*Cell culture.* Human bladder tumor-derived EJ-p53 cells, containing a tetracycline (tet)-regulated wild-type p53, were generated and maintained as previously described (1). For mitochondrial studies, cells were seeded onto glass coverslips at a density of $1 \times 10^5$ cells per 100-mm dish. EJ-p53 cells were induced to express p53 by removing tet from the growth media (1). EJ-p53 (−)tet refers to EJ-p53 cells that have been incubated in media without tet for 5 days, thereby allowing p53 to be induced, which subsequently triggers the senescence program. EJ-p53 (+)tet refers to cells maintained in media containing tet and therefore, do not express p53. EJ-p53 (+)tet and EJ-p53 (−)tet cells were treated with CSA (Sigma) at $10^{-7}$ M for 12 h.

PC12 cells (American Type Culture Collection, Rockville, MD) were cultured as previously described (27). Briefly, undifferentiated PC12 cells were maintained in Eagle's minimum essential medium (MEM) containing 10% horse serum, 5% fetal bovine serum, 2 mM L-glutamine (Life Technologies), 50 U/ml penicillin, and 50 ng/ml streptomycin (all from GIBCO BRL, Gaithersburg, MD). The PC12 cells were plated onto poly-L-lysine (Sigma)-coated glass coverslips and differentiated in MEM containing 100 ng/ml 7S nerve growth factor (NGF) (Upstate Biotechnology, Inc., Lake Placid, NY) with serum (MEM with serum and NGF, M/S + N) for 6 days. After 6 days in M/S + N, the PC12 cells showed a neuronal phenotype (26) and based on immunoreaction with a Ki-67 antibody (Novocastra, Newcastle upon Tyne, UK) more than 96% had left the cell cycle and were quiescent (Rideout, Mammen and Tatton, unpublished results). To induce apoptosis by withdrawing serum and NGF, the differentiated PC12 cells were washed three times with Hank's balanced salt solution (GIBCO BRL) before placement into MEM without serum and NGF (MEM only, M/O). The cells were examined at 6 h after washing, which was found to be the time point at which increased apoptotic nuclear degradation was first detected (27). CSA was added at a final concentration of $10^{-7}$ M to both the cultures for 6 h in M/S + N and M/O after the washing was completed. Of note, western blots and immunocytochemistry showed transient induction of p53 protein levels in the pre-apoptotic PC12 cells after withdrawal of serum and NGF (Carlile, Sugrue and Tatton, unpublished observations) in keeping with reports that NGF withdrawal results in p53-dependent apoptosis (28).

*Estimation of $\Delta\Psi_M$ using chloromethyl-tetramethylrosamine methyl ester (CMTMR).* CMTMR (Mitotracker Orange; Molecular Probes, Eugene, OR, (see refs. 2, 23, 27 for details, justification, and examples of our previous use of the dye) enters mitochondria of living cells proportionally to the negative charge difference between the cytoplasm and the mitochondrial matrix and therefore, estimates $\Delta\Psi_M$. CMTMR binds irreversibly to mitochondrial matrix thiols and can be fixed for immunocytochemical localization of proteins in the same cells that have been previously exposed to CMTMR. Due to the thiol binding, CMTMR fluorescence represents the highest level of negativity difference in the mitochondria during exposure to the dye. Estimations of $\Delta\Psi_M$ found using CMTMR have been shown to be proportional to those found in the same cells with other dual fluorescing $\Delta\Psi_M$-sensitive probes, like JC-1 (27), and to decrease in response to PTP opening caused by agents like atractyloside (23). 50

**FIG. 2.** Images of CMTMR fluorescence and biotin immunoreaction in control vs. senescent EJ-p53 cells. (A, B1) Gray scale, laser scanning confocal microscope images of typical control, EJ-p53 (+)tet cells, and (C, D1) of senescent, EJp53 (−)tet cells stained with CMTMR. A and C are low power images (all scale bars are 10 $\mu$m in length), while B1–B3 and D1–D3 are high power images centered on the cells marked by arrows in A and C, respectively. Note the lower level of CMTMR fluorescence in the senescent EJp53 (−)tet cells compared to the (+)tet cells, which is indicative of reduced $\Delta\Psi_M$. B3 (B1 and B2 added) and D3 (D1 and D3 added) are re-colored and digitally added images as in Fig. 1. Note that the levels of biotin immunoreaction is similar for the (+)tet and (−)tet cells but the shift in preponderant mitochondrial coloration from yellow-orange in B3 to yellow-green in D3 shows that biotin remains localized to mitochondria in spite of a $\Delta\Psi_M$ shift to lower levels in the (−)tet cells.

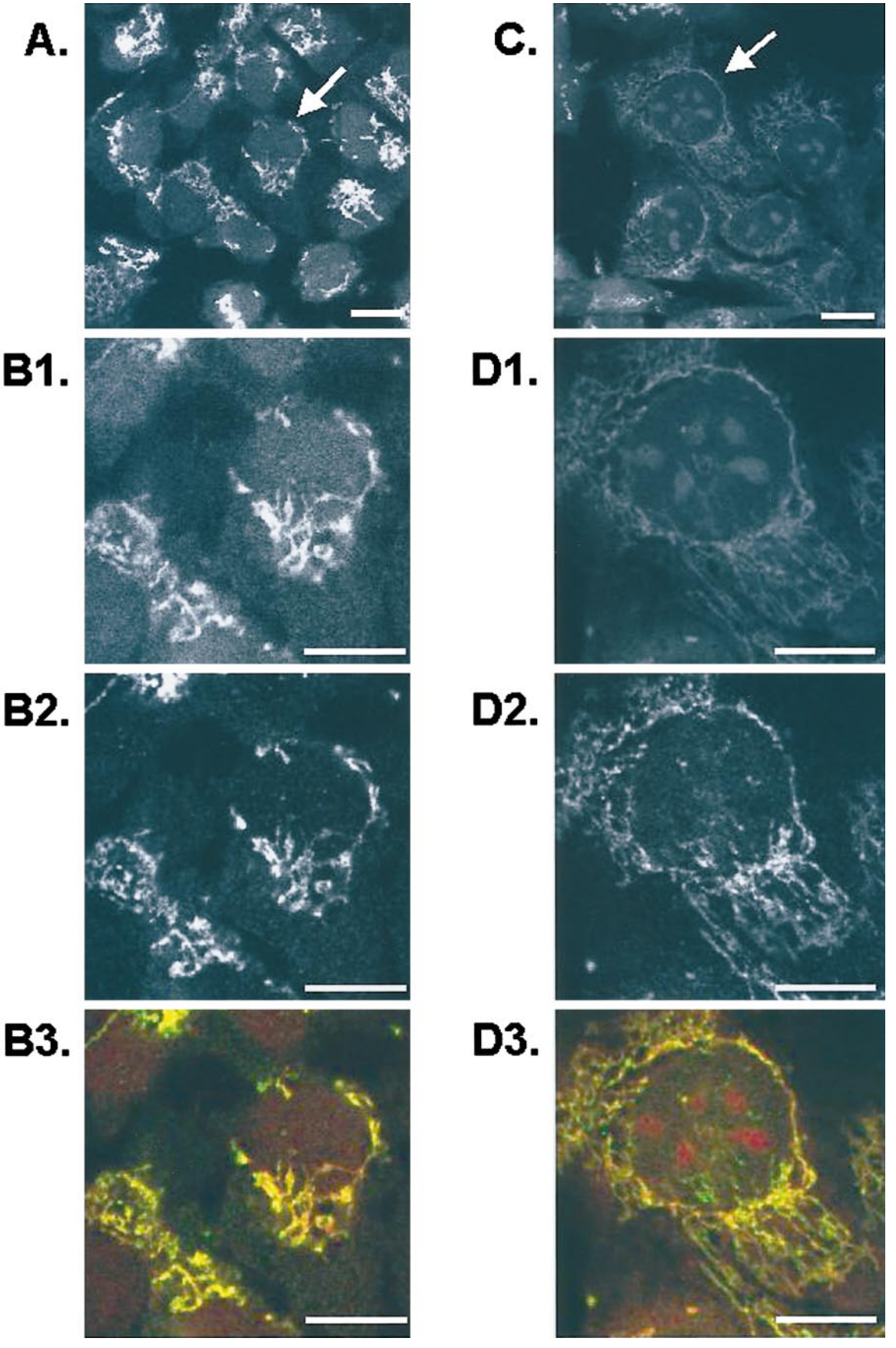
A.
C.
B1.
D1.
B2.
D2.
B3.
D3.

nM CMTMR was added directly to the media of EJ-p53 cells and the PC12 cells seeded on coverslips and incubated for 15 min at 37°C. The CMTMR-containing media was removed and the cells were rinsed with cold PBS, followed by immediate fixation with 4% paraformaldehyde on ice for 10 minutes. After fixation, the cells were rinsed with PBS and the coverslips were mounted onto microscope slides using Aquamount (GURR, England).

CMTMR fluorescence was imaged using a laser scanning confocal microscope (LSCM) as previously described (23, 27) All cells were imaged at the same level of laser intensity, detector sensitivity, and pinhole size in order to insure that CMTMR fluorescence intensity could be compared among different coverslips and treatments. The images were saved as TIFF files and then analyzed for mitochondrial fluorescence intensity using Metamorph software (Universal Imaging Corporation, West Chester, PA). Cells were chosen randomly and CMTMR fluorescence intensity values were measured from 20–30 different mitochondria/cell × 10 cells for each treatment from three different experiments. The values for each treatment were combined and presented as frequency distributions (~600 different individual mitochondrial measurements/histogram).

*Immunocytochemistry for biotin, a marker of mitochondria.* Biotin is covalently linked to four cellular carboxylases (28), three of which are located in mitochondria (propional CoA carboxylase, methyl-crotonyl-CoA carboxylase, and pyruvate carboxylase). It has been shown that antibodies against biotin selectively stain mitochondria (29). In previous work (27), we used more than one mitochondrial potentiometric dye to insure that subcellular changes in fluorescence were in fact generated from mitochondria. In this study, biotin antibodies were used as a means of ensuring that the subcellular elements showing CMTMR fluorescence were mitochondria. Cells on coverslips, previously incubated with CMTMR and fixed as described above, were permeabilized in 100% methanol at −20°C for 30 sec. Cells were then blocked with 10% normal goat serum (Jackson Immunoresearch Laboratories, Inc., West Grove, PA) in PBS at room temperature for 20 min. Incubation with an anti-biotin monoclonal antibody (Jackson Immunoresearch Laboratories, Inc.), diluted 1:100 in 1% goat serum/PBS, was performed at 4°C for 12 h. After rinsing with PBS, cells were incubated in secondary antibody, Cy5-labelled goat anti-mouse IgG (Jackson Immunoresearch Laboratories, Inc.), diluted 1:250 in 1% goat serum/PBS, at room temperature for 1 h in the dark. Finally, coverslips were rinsed in PBS and then mounted onto microscope slides using glycerol and sealed with clear nail polish. The procedure allowed the same mitochondria to be laser confocal imaged at two different wavelengths for biotin immunoreaction and CMTMR sequestration in order to determine whether mitochondria were the only elements with detectable CMTMR fluorescence and whether all mitochondria had $\Delta\Psi_M$.

*Statistical analysis.* To evaluate the data, the individual measurements from different treatment groups were first analyzed using Statistica software (StatSoft) using the Mann–Whitney U test (see ref. 27 for details and rationale of using a nonparametric test for the CMTMR data).

## RESULTS

*Biotin immunoreactivity co-localizes with CMTMR staining in mitochondria.* Figure 1 shows typical laser scanning confocal microscope (LSCM) images of CMTMR fluorescence and biotin immunoreactivity in PC12 cells maintained in NGF- and serum-supported, M/S + N (Fig. 1A1–A3) and in NGF- and serum-withdrawn, M/O (Fig. 1B1–B3) conditions. Coloring the CMTMR fluorescence red (Figs. 1A1; 1B1) and the biotin immunofluorescence green (Figs. 1A2; 1B2) followed by digital addition of the images (Figs. 1A3; 1B3) showed that relative levels of CMTMR fluorescence and biotin concentration varied between different mitochondria in the trophically supported and the trophically withdrawn PC12 cells. However, the subcellular loci of CMTMR fluorescence were always superimposed with biotin immunoreactivity. In contrast, biotin immunoreaction was present in subcellular structures without CMTMR fluorescence suggesting that those mitochondria had lost $\Delta\Psi_M$ but retained biotin immunoreactivity. Thus, CMTMR fluorescence (Fig. 1A1, 1B1) was co-localized with biotin immunoreaction (Fig. 1A2, 1B2) showing that the CMTMR-fluorescing elements were mitochondria.

*p53-overexpressing, senescent cells exhibit decreased $\Delta\Psi_M$.* Using CMTMR fluorescence to reflect $\Delta\Psi_M$ together with biotin immunoreactivity to label mitochondria, we performed double labeling experiments on EJ-p53 cells. Figure 2 shows typical laser confocal micrographs of CMTMR fluorescence in control, EJ-p53 (+)tet cells (Figs. 2A, 2B1), and in p53-overexpressing, senescent EJ-p53 (−)tet cells (Figs. 2C, 2D1). CMTMR fluorescence was considerably reduced in the senescent EJ-p53 (−)tet cells compared to the control EJ-p53 (+)tet cells (compare Figs. 2A and 2C and also Figs. 2B1 and 2D1). Despite the lower CMTMR fluorescence in senescent (−)tet cells, the levels of biotin immunofluorescence were similar in the (−)tet and (+)tet cells (compare Figs. 2B2 and 2D2). Similar to that for the PC12 cells (Fig. 1), red (CMTMR fluorescence)-green (biotin immunoreaction) re-coloring and combination of the images showed that CMTMR fluorescing elements were mitochondria in the EJ-p53 cells (Figs. 2B3, 2D3) and that relative levels of CMTMR fluorescence and biotin immunoreaction varied between different mitochondria in the control, EJ-p53 (+)tet cells and the senescent, EJ-p53 (−)tet cells.

*In situ laser scanning confocal microscope (LSCM) measurements of CMTMR fluorescence reflect $\Delta\Psi_M$.* Before we performed quantitative analyses of the CMTMR fluorescence in pre-apoptotic and senescent cells vs. control, we first examined the relationship between CMTMR fluorescence and PTP opening in *in situ* mitochondria imaged using LSCM. To accomplish this, we measured CMTMR fluorescence in neuronally differentiated PC12 cells treated with varying concentrations of atractyloside (ATR), which opens the PTP and dissipates the transmembrane proton gradient and, therefore, decreases $\Delta\Psi_M$ (30, 31). Figures 3A1, A2 show the CMTMR fluorescence in PC12 cells exposed to increasing concentrations of ATR. The addition of ATR to these cells caused a concentration-dependent decrease in mitochondrial CMTMR fluorescence and, therefore, established that LSCM-measured CMTMR fluorescence varies inversely with PTP opening and the dissipation of $\Delta\Psi_M$.

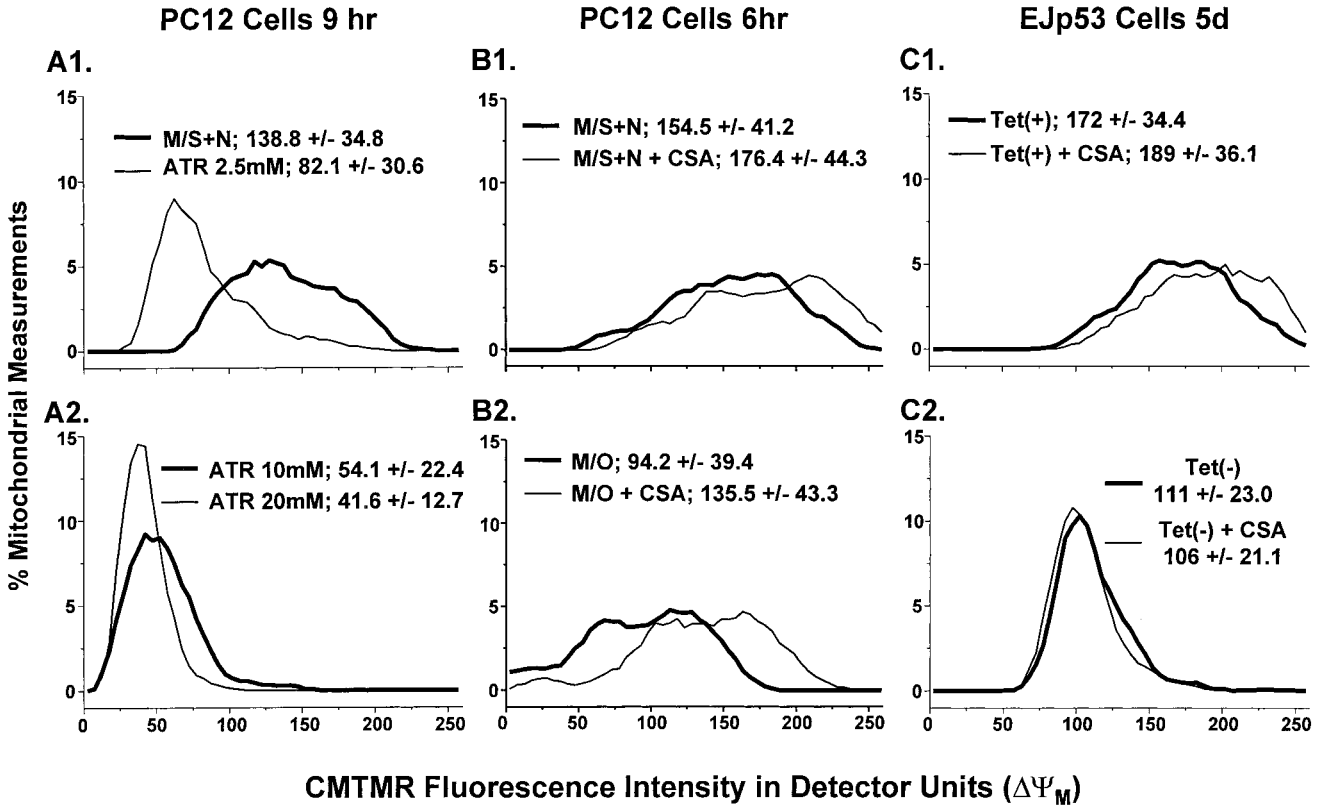


**FIG. 3.** CMTMR estimation of $\Delta\Psi_M$ in neuronally differentiated PC12 cells and in EJ-p53 cells. Numerical values superimposed on these and other distributions represent the mean and standard deviation for each distribution. (A1, A2) Distributions of *in situ* LSCM measurements of CMTMR fluorescence in neuronally differentiated PC12 cells stained with CMTMR and treated with varying concentrations of atractyloside (ATR). The thick line in A1 shows a typical CMTMR fluorescence distribution in PC12 cells supported by serum and NGF. The addition of increasing concentrations of ATR, which dissipates $\Delta\Psi_M$ by inducing sustained opening of the mitochondrial PTP, causes a progressive shift of the $\Delta\Psi_M$ distributions to lower levels (thin line in A1 and the thick and thin line in A2. These results are consistent with an increasing proportion of mitochondria having dissipated their $\Delta\Psi_M$ due to an increasing probability of sustained PTP opening. Moreover, these data demonstrate the $\Delta\Psi_M$ sensitivity of CMTMR fluorescence measured with LSCM. (B1, B2) Distributions of the CMTMR fluorescence for control PC12 cells that were replaced into serum and NGF (M/S+N, B1-thick line) compared to serum- and NGF-withdrawn (pre-apoptotic) PC12 cells (M/O, B2-thick line). The decrease in $\Delta\Psi_M$ as estimated by CMTMR fluorescence for the serum- and NGF-withdrawn PC12 cells (M/O, B3) compared to the control cells that were replaced into serum and NGF is typical of cells in the early phases of apoptosis (see refs. 12 and 27). CSA at $10^{-7}$ M increased CMTMR fluorescence for both the control cells (B1-thin line) and the serum- and NGF-withdrawn cells (B2-thick line). (C1, C2) Distributions of CMTMR fluorescence for EJ-p53 (+)tet (C1) and senescent EJ-p53 (−)tet cells (C2). CMTMR fluorescence was decreased in the senescent EJ-p53 (−)tet cells at 5 days (C2-thick line) compared to the EJ-p53 (+)tet cells at the same time point (C1-thick line). CSA at $10^{-7}$ increased CMTMR fluorescence in the EJ-p53 (+)tet cells (compare thick and thin lines in C1) but did not alter the reduced CMTMR fluorescence for EJ-p53 (−)tet cells (compare thick and thin lines in C2).

*NGF and serum withdrawn PC12 cells show decreased $\Delta\Psi_M$, which is increased by treatment with cyclosporin A.* Similar to that previously reported (27), the pre-apoptotic PC12 cells, which had been NGF- and serum-withdrawn by placement in M/O 6 hours previously (Fig. 3B2), showed a shift in the distribution of CMTMR fluorescence, and therefore $\Delta\Psi_M$, to significantly lower levels ($P > 0.001$) than those for cells, which were similarly washed to remove serum and NGF but were then replaced in M/S+N (Fig. 3B1). We then determined whether $\Delta\Psi_M$ in the PC12 cells could be affected by CSA, which facilitates closure of the PTP and thereby increases $\Delta\Psi_M$ (22, 23). We treated the washed PC12 cells in M/S + N and M/O with $10^{-7}$ M CSA for 6 h. Treatment of the PC12 cells in both the trophically supported condition (M/S + N) and those in the trophically withdrawn/pre-apoptotic condition (M/O) with $10^{-7}$ M CSA shifted the CMTMR fluorescence distribution to higher levels (compare Figs. 3B1, (+) vs. (−) CSA, $p < 0.05$ and Figs. 3B2, (+) vs. (−) CSA, $p < 0.01$), in a manner similar to that previously reported for PC12 cells (23) and other cells with decreased $\Delta\Psi_M$ (22, 23).

*CMTMR fluorescence as estimate of $\Delta\Psi_M$ is decreased in senescent EJ-p53 cells.* Distributions of $\Delta\Psi_M$, as estimated by measurements of mitochondrial CMTMR fluorescence, were significantly shifted to lower levels in senescent EJ-p53 (−)tet cells as compared to control, EJ-p53 (+)tet cells (compare distribution in Fig. 3C1 to

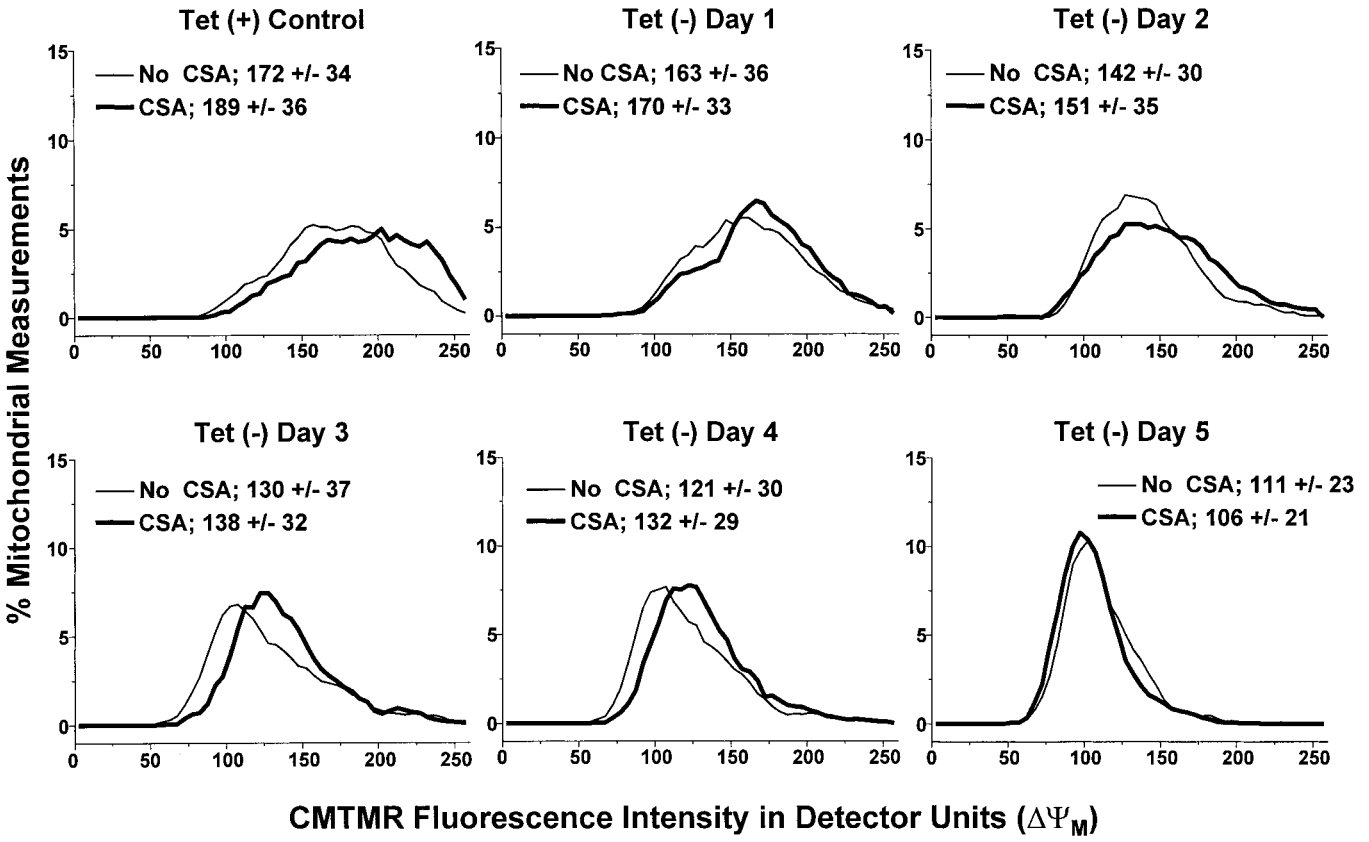


**FIG. 4.** Temporal progression of decreased $\Delta\Psi_M$ and reduced CSA responsiveness in EJ-p53 (−)tet cells. Distributions for estimated $\Delta\Psi_M$ in senescent EJ-p53 (−)tet cells at days 1 through 5 after the removal of tet. In each pair of distributions, the thick line is for cells treated with $10^{-7}$ M CSA and the thin line is for untreated cells. Note the gradual shift of CMTMR fluorescence to lower levels for each successive day in (−)tet coupled with a gradual loss of the increased in CMTMR fluorescence induced by the CSA treatment. The progression of these changes is similar in terms of time frame to that previously reported for the progression of the senescent phenotype in the EJ-p53 (−)tet cells (1).

that in Fig. 3C2, $p < 0.001$). Furthermore, there was a narrower distribution of CMTMR fluorescence in the senescent EJ-p53 (−)tet cells (Fig. 3C2). Of note, we have found similarly decreased levels of $\Delta\Psi_M$, as measured by CMTMR fluorescence, in human diploid fibroblast IMR-90 cells undergoing natural senescence (data not shown).

*CSA treatment does not block the dissipation of $\Delta\Psi_M$ observed in senescent EJ-p53 cells.* Given the similarity in the pre-apoptotic PC12 cells and the senescent EJ-p53 (−)tet cells in terms of decreased $\Delta\Psi_M$ compared to control, we wanted to analyze the effect of CSA on $\Delta\Psi_M$ in EJ-p53 cells. We treated EJ-p53 (+)tet and (−)tet cells, with $10^{-7}$ M CSA for 12 h. Similar to the results reported above with PC12 cells, the CSA treatment caused a significant shift of the CMTMR fluorescence distributions to higher levels in control cells, EJ-p53 (+)tet, (compare Figs. 3C1, (+) vs. (−) CSA, $p < 0.05$). However, CSA did not significantly alter the CMTMR fluorescence distribution in the senescent EJ-p53 (−)tet cells (compare Figs. 3C2, (+) vs. (−) CSA, $p > 0.05$).

*Decreased $\Delta\Psi_M$ and decreased responsiveness to CSA are temporally correlated with the commitment to senescence in EJ-p53 cells.* We also performed a time course experiment in which EJ-p53 cells were treated with CSA at different time points after the removal of tet induction of p53. Figure 4 shows the progressive decrease in the CMTMR fluorescence for EJ-p53 (−)tet cell mitochondria, which became significant at day 2, when compared to the distribution for the EJ-p53 (+)tet cells ($p < 0.05$), and progressively decreased over the following three days. As also shown in Fig. 4, at days 1 and 2 following the removal of tet from the EJ-p53 cells, there was a small but significant (p's $<$ 0.05) increase in CMTMR fluorescence in response to CSA treatment (no CSA-thin line; (+) CSA-thick line), but there was not a significant increase at days 3, 4 or 5 (p's $> 0.05$). Of note, the senescence phenotype in EJ-p53 (−)tet cells is irreversible by 2-3 days after tet is removed(1). Thus, both the decreased $\Delta\Psi_M$ distribution and the loss of capacity of CSA to increase $\Delta\Psi_M$ in the EJ-p53 (−)tet cells are temporally correlated with the commitment to senescence in EJ-p53 cells.

## DISCUSSION

Our results indicate that a decrease in $\Delta\Psi_M$ is characteristic of cells entering senescence after p53 overexpression. The decrease seems similar to that previously found in several types of aging cells (3–9). It is uncertain as to how p53 overexpression might dissipate $\Delta\Psi_M$. Decreases in $\Delta\Psi_M$ can result from ionic redistribution across the inner mitochondrial membrane, eg. an increase in intramitochondrial $Ca^{2+}$ levels (27); decreases in outward proton pumping across the inner mitochondrial membrane, such as that caused by toxins to the mitochondrial respiratory complexes (23, 32); agents which increase the lipid permeability of the inner mitochondrial membrane (33); or factors which promote sustained opening of the PTP (23, 34).

The PTP consists of a number of proteins, including the adenine nucleotide translocator (ANT), a voltage-dependent anion channel (VDAC), hexokinase, creatine kinase, and a peripheral benzodiazepine binding protein (see ref. 13 for a review of the components of the PTP and the factors or agents that influence its opening and closing). A decrease in $\Delta\Psi_M$ with a concomitant decrease in the proton gradient across the inner mitochondrial membrane causes cyclophilin D to bind to ANT with subsequent opening of the PTP (21, 24, 25). Recent evidence suggests that ANT is involved in the formation of the pore (35–38).

Both the decrease in $\Delta\Psi_M$ and the inability of CSA to increase $\Delta\Psi_M$ in the p53-induced senescent cells could result from p53 or one of several p53-induced gene products directly or indirectly interfering with ANT or another element of the PTP. For example, the anti-apoptotic oncoprotein, BCL-2, localizes to the outer mitochondrial membrane where it facilitates PTP closure (39–41). Conversely, the pro-apoptotic molecule BAX binds to ANT and increases PTP permeability (42–43). p53 induces an increase in BAX synthesis and a decrease in BCL-2 synthesis in many cells entering apoptosis (44–45). We have also detected an increase in BAX expression in EJ-p53 (−)tet cells after p53 is induced (Lee and Sugrue, unpublished observations). Thus, increased BAX levels resulting from p53 overexpression might explain the decreased $\Delta\Psi_M$ and decreased CSA responsiveness in the senescent EJ-p53 (−)tet cells. That is, the decrease in $\Delta\Psi_M$ could result from proton leakage across the PTP modulated by BAX. Alternatively, the recent report of decreased expression of ANT in senescent human diploid fibroblasts cells in culture (46) might be expected to result in decreased or absent CSA responsiveness and thereby, help to explain our findings.

We have previously demonstrated that EJ-p53 cells do not become irreversibly committed to the senescent program until 2–3 days after tet removal with concomitant p53 expression (1). Temporally, the decrease in $\Delta\Psi_M$ and the decreased CSA-responsiveness observed in EJ-p53 cells occurs gradually over the same time period as the commitment to senescence. Given that the appearance of the decreased $\Delta\Psi_M$ and the decrease in CSA responsiveness are concomitant with the establishment of the senescence phenotype, it is possible that these mitochondrial changes contribute to the causal factors that establish the senescence phenotype. Despite the temporal correlation, it can also be argued that the decrease in $\Delta\Psi_M$ and the decrease in CSA responsiveness are merely a result of senescence and are not contributors to its evolution. Experiments in which $\Delta\Psi_M$ and/or PTP components are chronically manipulated pharmacologically or genetically will be required to determine whether components of the mitochondrial membrane megachannel contribute to senescence in EJ-p53 (−)tet cells.

## ACKNOWLEDGMENTS

This work was supported in part by National Institutes of Health Grant K08CA72969, Bear Necessities Pediatric Cancer Foundation Grant, and Lehman Brothers Grant (to M.M.S.) and a Lowenstein Foundation Grant (to W.G.T.).

## REFERENCES

1. Sugrue, M. M., Shin, D. Y., Lee, S. W., and Aaronson, S. A. (1997) *Proc. Natl. Acad. Sci. USA* **94,** 9648–9653.
2. Grant, S. M., Shankar, S. L., Chalmers-Redman, R. M., Tatton, W. G., Szyf, M., and Cuello, A. C. (1999) *Neuroreport* **10,** 41–46.
3. Hagen, T. M., Yowe, D. L., Bartholomew, J. C., Wehr, C. M., Do, K. L., Park, J. Y., and Ames, B. N. (1997) *Proc. Natl. Acad. Sci. USA* **94,** 3064–3069.
4. Lopez-Mediavilla, C., Orfao, A., San Miguel, J., and Medina, J. M. (1992) *Exp. Cell Res.* **203,** 134–140.
5. Martinez, A. O., Over, D., Armstrong, L. S., Manzano, L., Taylor, R., and Chambers, J. (1991) *Growth Dev. Aging* **55,** 185–191.
6. Rottenberg, H., and Wu, S. (1997) *Biochem. Biophys. Res. Commun.* **240,** 68–74.
7. Pieri, C., Recchioni, R., and Moroni, F. (1993) *Mech. Aging Dev.* **70,** 201–212.
8. Leprat, P., Ratinaud, M. H., and Julien, R. (1990) *Mech. Aging Dev.* **52,** 149–167.
9. Linnane, A. W., Degli Esposti, M., Generowicz, M., Luff, A. R., and Nagley, P. (1995) *Biochim. Biophys. Acta* **1271,** 191–194.
10. Susin, S. A., Zamzami, N., and Kroemer, G. (1996) *Apoptosis* **1,** 231–242.
11. Marchetti, P., Castedo, M., Susin, S. A., Zamzami, N., Hirsch, T., Macho, A., Haeffner, A., Hirsch, F., Geuskens, M., and Kroemer, G. (1996) *J. Exp. Med.* **184,** 1155–1160.
12. Susin, S. A., Zamzami, N., and Kroemer, G. (1998) *Biochim. Biophys. Acta Bioenergetics* **1366,** 151–165.
13. Tatton, W. G., and Olanow, C. W. (1999) *Biochim. Biophys. Acta* **1410,** 195–213.
14. Marzo, I., Brenner, C., and Kroemer, G. (1998) *Biomed. Pharmacother.* **52,** 248–251.
15. Heiskanen, K. M., Bhat, M. B., Wang, H. W., Ma, J., and Nieminen, A. L. (1999) *J. Biol. Chem.* **274,** 5654–5658.
16. Susin, S. A., Lorenzo, H. K., Zamzami, N., Marzo, I., Brenner, C., Laorchette, N., Prevost, M. C., Alzari, P. M., and Kroemer, G. (1999) *J. Exp. Med.* **189,** 381–393.

17. Yang, J. C., and Cortopassi, G. A. (1998) *Free Radical Biol. Med.* **24,** 624–631.
18. Susin, S. A., Lorenzo, H. K., Zamzami, N., Marzo, I., Snow, B. E., Brothers, G. M., Mangion, J., Jacotot, E., Costantini, P., Loeffler, M., Larochette, N., Goodlett, D. R., Aebersold, R., Siderovski, D. P., Penninger, J. M., and Kroemer, G. (1999) *Nature* **397,** 441–446.
19. Kroemer, G., Dallaporta, B., and Resche-Rigon, M. (1998) *Annu. Rev. Physiol.* **60,** 619–642.
20. Bernardi, P. (1996) *Biochim. Biophys. Acta* **1275,** 5–9.
21. Scorrano, L., Nicolli, A., Basso, E., Petronilli, V., and Bernardi, P. (1997) *Mol. Cell Biochem.* **174,** 181–184.
22. Cassarino, D. S., Swerdlow, R. H., Parks, J. K., Parker, W. E., Jr., and Bennett, J. P. Jr. (1998) *Biochem. Biophys. Res. Commun.* **248,** 168–173.
23. Chalmers-Redman, R. M. E., Fraser, A. D., Carlile, G. W., Pong, A., and Tatton, W. G. (1999) *Biochem. Biophys. Res. Commun.* **257,** 440–447.
24. Woodfield, K., Ruck, A., Brdiczka, D., and Halestrap, A. P. (1998) *Biochem. J.* **336**(pt 2), 287–290.
25. Crompton, M., Virji, S., and Ward, J. M. (1998) *Eur. J. Biochem.* **258,** 729–735.
26. Tatton, W. G., Ju, W. Y., Holland, D. P., Tai, C., and Kwan, M. (1994) *J. Neurochem.* **63,** 1572–1575.
27. Wadia, J. S., Chalmers-Redman, R. M. E., Ju, W. J. H., Carlile, G. W., Phillips, J. L., and Tatton, W. G. (1998) *J. Neurosci.* **18,** 932–947.
28. Scriver, C. R., Beaudet, A. L., Sly, W. S., and Valle, D. (1995) Metabolic and Molecular Basis of Inherited Disease. McGraw–Hill, New York, NY.
29. Hollinshead, M., Sanderson, J., and Vaux, D. J. (1997) *J. Histochem. Cytochem.* **45,** 1053–1057.
30. Fall, C. P., and Bennett, J. P. (1999) *Biochim. Biophys. Acta* **1410,** 77–84.
31. Zamzami, N., Marchetti, P., Castedo, M., Hirsh, T., Susin, S. A., Masse, B., and Kroemer, G. (1996) *FEBS Lett.* **384,** 53–57.
32. Wu, E. Y., Smith, M. T., Bellomo, G., and Di Monte, D. (1990) *Arch. Biochem. Biophys.* **282,** 358–362.
33. Schonfeld, P., Schild, L., and Kunz, W. (1989) *Biochim. Biophys. Acta* **977,** 266–272.
34. Halestrap, A. P., Woodfield, K. Y., and Connern, C. P. (1997) *J. Biol. Chem.* **272,** 3346–3354.
35. Ruck, A., Dolder, M., Wallimann, T., and Brdiczka, D. (1998) *FEBS Lett.* **426,** 97–101.
36. Beutner, G., Ruck, A., Riede, B., and Brdiczka, D. (1998) *Biochim. Biophys. Acta* **1368,** 7–18.
37. Zazueta, C., Reyes-Vivas, H., Zafra, G., Sanchez, C. A., Vera, G., and Chavez, E. (1998) *Int. J. Biochem. Cell Biol.* **30,** 517–527.
38. deMacedo, D. V., da Costa, C., and Pereira-Da-Silva, L. (1997) *Comp. Biochem. Physiol. B Biochem. Mol. Biol.* **118,** 209–216.
39. Shimizu, S., Eguchi, Y., Kamiike, W., Waguri, S., Uchiyama, Y., Matsuda, H., and Tsujimoto, Y. (1996) *Oncogene* **13,** 21–29.
40. Zamzami, N., Brenner, C., Marzo, I., Susin, S. A., and Kroemer, G. (1998) *Oncogene* **16,** 2265–2282.
41. Marzo, I., Brenner, C., Zamzami, N., Susin, S. A., Beutner, G., Brdiczka, D., Remy, R., Xie, Z., Reed, J. C., and Kroemer, G. (1998) *J. Exp. Med.* **187,** 1261–1271.
42. Marzo, I., Brenner, C., Zamzami ,N., Jurgensmeier, J. M., Susin, S. A., Vieira, H. L., Prevost, M. C., Xie, Z., Matsuyama, S., Reed, J. C., and Kroemer, G. (1998) *Science* **281,** 2027–2031.
43. Narita, M., Shimizu, S., Ito, T., Chittenden, T., Lutz, R. J., Matsuda, H., and Tsujimoto, Y. (1998) *Proc. Natl. Acad. Sci. USA* **95,** 14681–14686.
44. Basu, A., and Haldar, S. (1998) *Mol. Hum. Reprod.* **4,** 1099–1109.
45. Bates, S., and Vousden, K. H. (1999) *Cell Mol. Life Sci.* **55,** 28–37.
46. Fan, W. M., Kou, H., Shen, D. J., and LeRoy, E. C. (1998) *Exp. Gerontol.* **33,** 457–465.